1 **Title:** Into the tropics: phylogenomics and evolutionary dynamics of a contrarian
2 clade of ants
3
4 RH: Evolution of the ant tribe Stenammini
5

6 Michael G. Branstetter[1,2], John T. Longino[1], Joaquín Reyes-López[3], Ted R. Schultz[2],
7 Seán G. Brady[2]
8
9 [1]Department of Biology, University of Utah, Salt Lake City, UT 84112, USA
10
11 [2]Department of Entomology, National Museum of Natural History, Smithsonian
12 Institution, Washington, D.C., 20560, USA
13
14 [3]Departamento de Botánica, Ecología y Fisiología Vegetal, Universidad de Córdoba,
15 Córdoba, Spain
16
17 Corresponding Author:
18 Michael G. Branstetter
19 Department of Biology, University of Utah, 257 S 1400 E, Salt Lake City, UT 84112,
20 USA, Email: mgbranstetter@gmail.com
21

24
25

ABSTRACT

Aim. The standard latitudinal diversity gradient (LDG), in which species richness decreases from equator to pole, is a pervasive pattern observed in most groups of organisms. Despite its commonness, an increasing number of non-conforming lineages have been identified, presenting a challenge for general explanations of the standard LDG. Although problematic, documenting and studying these contrarian groups can help us to better understand LDGs generally. To that end we identify the ant tribe Stenammini, a diverse lineage with over 400 species, as a contrarian clade, and we attempt to explain the group's atypical diversity pattern using a historical approach. We evaluate the following alternative hypotheses: time-for-speciation/center-of-origin (TFS/COO), niche conservatism, and differences in diversification rate.

Location. Global.

Methods. We examine the shape of the LDG in Stenammini by plotting latitudinal midpoints for all extant species. We then infer a robust phylogeny using a phylogenomic approach that employs ultraconserved element loci and we use the phylogeny to estimate divergence dates, biogeographic history, and ancestral habitats. We also test for diversification rate heterogeneity across the tree and among lineages within the tribe.

Results. Stenammini has a skewed inverse latitudinal diversity gradient with an extratropical richness peak in the northern temperate zone. Our phylogenomic

51   approach resulted in a robust phylogeny revealing five major clades and several

52   instances of non-monophyly among genera (*Goniomma*, *Aphaenogaster*). The tribe

53   and most major lineages originated in the temperate zone and inhabited temperate

54   niches. Crown Stenammini dates to 52 Ma (Eocene Climatic Optimum) and most

55   major lineages appeared soon after during a period of global cooling. Despite its

56   temperate origin, the group invaded the tropics at least six times, but failed to

57   diversify greatly there. Across the tree diversification increased from 17.2-1.9 Ma

58   following the Mid-Miocene Climatic Optimum, and among lineages there was a rate

59   increase in Holarctic *Aphaenogaster* + *Messor* just prior to 17.2 Ma.

60

61   **Main Conclusions.** Our results suggest that time, niche conservatism, and increased

62   diversification have all contributed to the inverse latitudinal gradient in Stenammini.

63   Among these processes, niche conservatism may be less important given that the tribe

64   has dispersed to the tropics multiple times.

65

66

67   **INTRODUCTION**

68

69   The observation that species richness decreases from equator to pole is the oldest and

70   best-known pattern in biogeography (Hawkins, 2001; Willig et al., 2003). Although

71   not a consistent pattern throughout the history of life on Earth, the current latitudinal

72   diversity gradient (LDG) has existed for at least the last 30 million years and is

73   pervasive (Mannion et al., 2013). The standard LDG occurs in most fauna and flora,

74   in both terrestrial and marine realms, and across a range of spatial and temporal scales

75   (Willig et al., 2003; Hillebrand, 2004; Field et al., 2009; Brown, 2014). Hypotheses

76   attempting to explain the standard LDG abound, yet a broad consensus as to which

77   hypothesis, or set of hypotheses, best predicts the gradient remains a topic of active

78   debate (Pianka, 1966; Rohde, 1992; Willig et al., 2003; Wiens & Donoghue, 2004;

79   Jablonski et al., 2006; Brown, 2014).

80

81   A challenge to understanding the standard LDG has been the discovery of a small but

82   growing number of lineages that exhibit inverse diversity gradients, in which species

83   richness peaks in extratropical regions and decreases toward the equator. These

84   contrarian clades occur in a variety of marine and terrestrial groups, including marine

85   bivalves (Krug et al., 2007), pelagic seabirds (Chown et al., 1998), ichneumonid

86   wasps (Owen & Owen, 1974), and lampropeltinine snakes (Pyron & Burbrink, 2009).

87   Seemingly problematic, discovery of these groups has actually improved our

88   understanding of diversity gradients, because it has made it necessary to explain these

89   non-standard cases using the same fundamental mechanisms (i.e., speciation,

90   extinction, and dispersal) that underlie the standard LDG. Thus, a productive goal in

91   biogeography should be to identify contrarian clades and to understand the ecological

92   and evolutionary processes that have caused them to be different. Here, we

93   demonstrate that a major group of ants is a contrarian clade and we infer a robust

94   phylogeny of the group to test several hypotheses that might account for the group's

95   atypical diversity pattern.

96

97   Ants (Hymenoptera, Formicidae) are the most successful group of eusocial insects on

98   Earth. They occur in most terrestrial ecosystems and are often ecologically and

99   numerically dominant (Hölldobler & Wilson, 1990). As a whole, ants exhibit the

100   standard LDG (Kaspari et al., 2003), with the Neotropics being particularly important

101   in the group's evolutionary history (Moreau & Bell, 2013). Several ant lineages,

102   however, are predominately temperate in distribution and exhibit obvious adaptations

103   to living in colder, seasonal environments. One of the largest of these groups is the

104   myrmicine ant tribe Stenammini (sensu Ward et al., 2015)

105

106   Stenammini is a monophyletic tribe that currently includes seven genera and over 400

107   extant species (Bolton, 2015). It occurs across the globe, being absent from only

108   Amazonia, temperate South America, and permanently frozen regions. Considering

109   type localities of described species, the majority of the tribe's diversity occurs in the

110   temperate zone of the northern hemisphere, with less than one quarter of the species

111   known from the New and Old World tropics, a pattern that strongly suggests an

112   inverse latitudinal gradient. Ecologically, the tribe exhibits a variety of life history

113   strategies, but the group is best known for several genera that have radiated in arid

114   landscapes as seed harvesters. These lineages are the genera *Messor, Veromessor,*

115   *Novomessor, Goniomma,* and *Oxyopomyrmex.* The remaining two genera in the tribe,

116 *Stenamma* and *Aphaenogaster*, are less specialized in their diets and are more

117 strongly associated with mesic forest habitats.

118

119 Among the seed harvester lineages the genus *Messor* is the most diverse. It includes

120 over 100 species and is distributed across the Palearctic and in arid regions

121 throughout Africa. The genus *Veromessor* includes only nine species and is restricted

122 to arid regions of the western United States and west-central Mexico (Johnson, 2001).

123 This genus was previously synonymized with *Messor* based on its deceptively similar

124 seed-harvester morphology (Bolton, 1982), but recent molecular analyses revealed

125 that the similarities are convergent and that the North American species are not

126 closely related to *Messor* (Brady et al., 2006; Ward et al., 2015). The genus

127 *Novomessor* includes only three species and occurs in the southwestern USA and

128 northern Mexico. It was previously synonymized with the genus *Aphaenogaster*

129 (Bolton, 1982), but was recently resurrected based on phylogenetic analyses that

130 included molecular data (Demarco & Cognato, 2015). Because it is less specialized

131 and scavenges on a diverse range of food items *Novomessor* does not have the seed-

132 harvester gestalt, but it is adapted to arid environments and forages on seeds as a

133 significant part of its diet (Whitford et al., 1980; Johnson, 2001). The last two seed-

134 harvester genera are *Goniomma* and *Oxyopomyrmex*. Both of these have large eyes

135 and forage for seeds at night. Together they include about 20 species and are

136 restricted to arid habitats around the Mediterranean region (Salata & Borowiec,

137 2015).

138

139 Of the remaining two members of Stenammini, *Aphaenogaster* is the largest and most

140 taxonomically problematic genus in the tribe. It currently includes over 180 described

141 species, distributed mostly throughout the Holarctic, but with some species diversity

142 in the Neotropical (Mexico, Central America, Haiti), Afrotropical (Madagascar),

143 Indomalayan, and Australasian regions. Within Australia, a few species penetrate into

144 the southern temperate zone. Although the genus *Novomessor* was recently

145 resurrected and removed from *Aphaenogaster*, considerable uncertainty remains as to

146 whether *Aphaenogaster* is monophyletic (Ward et al., 2015). The group shows

147 considerable morphological diversity and includes a number of genus-level names

148 that are currently synonymized under *Aphaenogaster* (Bolton, 2015). Ecologically,

149 the majority of species are scavengers that inhabit forested regions in the temperate

150 zone, but a number of species have penetrated into arid and rainforest habitats in both

151 the New and Old Worlds. Morphologically, one of the more striking features in the

152 genus is the tendency for tropical species to become large and elongate, with the

153 posterior end of the head extending into a long neck (e.g., *A. dromedaria*).

154

155 The genus *Stenamma* is the third largest member of the tribe with just over 80

156 described species. It occurs throughout the Holarctic and partway into the Neotropics,

157 reaching as far south as northern South America (Branstetter, 2009, 2012, 2013). The

158 genus differs from the rest of the tribe in that it is composed primarily of small-sized,

159 cryptic ants that are most often found in the leaf litter of forested regions. Recent

160 molecular work has demonstrated that the genus is monophyletic and that it is divided

161 into equally diverse Holarctic and Neotropical clades (Branstetter, 2012). It also

162 determined that the genus likely originated in the Nearctic and dispersed into the

163 Neotropics, where it radiated in montane wet forests. Although the genus does not

164 have an inverse latitudinal gradient, it does represent a contrasting example to the out-

165 of-the tropics hypothesis, which proposes that most lineages evolved in the tropics

166 and dispersed out (Jablonski et al., 2006).

167

168 The fossil record for Stenammini is seemingly rich (Bolton, 2015), including 18

169 putative species of *Aphaenogaster*, one species of *Stenamma*, one species of *Messor*

170 (currently an unresolved junior homonym), and four species of a possibly related

171 genus *Paraphaenogaster*. However, this richness belies the fact that the placement of

172 many of these fossil taxa within the tribe, or within genera in the tribe, is dubious,

173 largely due to uncertainty in both diagnostic characters and generic boundaries.

174 Considering reliable fossils, the tribe has been documented from the Eocene Period

175 onwards, with records from various Eurasian deposits, including Baltic Amber

176 (Wheeler, 1915), and several New World deposits, including the Florrisant Shale of

177 Colorado (Carpenter, 1930), and the Dominican and Chiapas Ambers (De Andrade,

178 1995). The overall record suggests the tribe has been present throughout the Holarctic

179 since the Eocene and in Central America since the late Oligocene.

180

181 In the present study we demonstrate that the ant tribe Stenammini is a biogeographic

182 contrarian, exhibiting an inverse latitudinal gradient. Following this observation we

183 take a historical approach, employing phylogenomic techniques and a variety of tree-

184 based comparative methods (e.g. divergence dating, ancestral area and habitat

185 reconstruction, and diversification rate-shift tests) to assess alternative hypotheses that

186 might explain the tribe's atypical diversity pattern. Specifically, we consider three

187 hypotheses that have been used to explain LDGs and that can be evaluated using tree-

188 based approaches. These are the time-for-speciation/center-of-origin (TFS/COO)

189 hypothesis (Schluter, 1993; Wiens & Donoghue, 2004; Stevens, 2006), the niche

190   conservatism hypothesis (Wiens & Donoghue, 2004; Wiens & Graham, 2005), and

191   the diversification rate hypothesis (Rohde, 1992; Cardillo et al., 2005; Weir &

192   Schluter, 2007). The TFS/COO proposes that species richness is primarily a function

193   of the time a particular lineage has been present in a region. Thus, if a lineage has

194   more species in the temperate zone, the prediction would be that the lineage

195   originated in the temperate zone and has had more time to evolve there. The niche

196   conservatism hypothesis proposes that niche evolution is rare, and a lineage with

197   more temperate diversity should have a temperate ancestor and few transitions into

198   the tropics and into tropical habitats. Lastly, the diversification rate hypothesis

199   proposes that differences in richness are due to differences in speciation and

200   extinction rates. Under this hypothesis, the region with more species should have

201   either a higher speciation rate or a lower extinction rate.

202

203   **MATERIALS AND METHODS**

204

205   **Assessing the Diversity Gradient**

206

207   To examine the latitudinal diversity gradient in Stenammini we estimated the

208   latitudinal midpoint for all extant described species in the tribe (see Appendix S1).

209   This was carried out by inspecting the distribution of every species using an online

210   database of ant species distributions (www.antmaps.org; Guénard et al., 2015) and

211   recording the northernmost and southernmost point for each. In cases where only an

212   administrative district was reported (country, state, *etc.*) rather than a point record, we

213   estimated the latitude as either the midpoint of the country, or, alternatively, of a

214   biogeographically sensible location. Using the midpoint latitudes we classified

215   species as having either tropical or extratropical distributions and we generated a

216   histogram of all points in R v3.2.2 (R Core Team, 2015).

217

218   **Phylogeny Taxon Selection**

219

220   We selected eight outgroup and 92 ingroup species for inclusion in our study (see

221   Appendix S2 for voucher information). Within Stenammini we included all genera

222   and a selection of exemplar species from all regions where each genus occurs. For

223   *Stenamma,* we included 23 species from the Neotropics and 14 species from the

224   Holarctic, including a rare species from Morocco (*S. punctiventre*) that has not been

225   sampled previously. We sampled all three species of the genus *Novomessor* and eight

226   out of the nine species of *Veromessor*. We sampled five out of eight species of

227   *Goniomma* and three out of 12 species of *Oxyopomyrmex*. For *Messor,* we only

228   sampled six species, but these included taxa from southern Africa, Europe, and Asia.

229   For *Aphaenogaster* we sampled 12 tropical species, nine Nearctic species, and nine

230   Palearctic species. The tropical species include three from the Neotropics, five from

231   Madagascar, one from Borneo, two from New Guinea, and one from Australia. One

232   interesting species of uncertain affinity that we were unable to sample is

233   *Aphaenogaster relicta*. Recorded from Haiti, it is the only known stenammine species

234   to occur in the Caribbean. Despite several recent collecting trips to Hispaniola by

235   colleagues, fresh material of this species was not acquired.

236

237   **Phylogeny Data Generation**

238

239 To generate a robust phylogeny we employed a recently developed phylogenomic

240 method that combines target enrichment of ultraconserved elements (UCEs) with

241 multiplexed next-generation sequencing (Faircloth et al., 2012, 2015). The approach

242 is preferable to more traditional Sanger sequencing because it results in orders of

243 magnitude more data in less time and at less cost. The steps for conducting the lab

244 work are the following: DNA extraction, library preparation, UCE enrichment, and

245 sequencing. The protocols are outlined in Faircloth et al. (2015) and given in detail

246 below. We extracted sequence data for 12 species from Faircloth et al. (2015) and

247 generated new sequence data for the remaining taxa.

248

249 For all newly sampled taxa, we extracted DNA using Qiagen DNeasy Blood and

250 Tissue kits (Qiagen Inc., Valencia, CA). We measured DNA concentration using a

251 Qubit 2.0 fluorometer (Life Technologies) and we input up to 500 ng of DNA into

252 shearing and library preparation. We sheared DNA to an average fragment

253 distribution of 400-600 bp (verified on an agarose gel) using a Qsonica Q800R

254 sonicator (Qsonica LLC, Newton, CT).

255

256 Following sonication, we constructed sequencing libraries using the standard Library

257 Preparation Kit or the newer Hyper Prep Kit from Kapa (Kapa Biosystems,

258 Wilmington, MA). We performed all reactions at ¼ volume except for the PCR step,

259 which we assembled at full volume (50 μL). During library preparation we added

260 custom, single-indexing Truseq-style barcode adapters to most samples (Faircloth &

261 Glenn, 2012). However, for a few libraries, we used a newer, dual-indexing set of

262 adapter-primers called iTru (Faircloth & Glen, pers. comm.). These adapters are

263 analogous to the Illumina TruSeq HT system and are added to the libraries during the

264 PCR step of library preparation. We assessed success of library preparation by

265 measuring DNA concentration with the Qubit flourometer and by visualizing the

266 libraries on an agarose gel. For a subset of the samples, we removed adapter-dimers

267 by performing a 0.7-0.8X SPRI-bead cleaning.

268

269 For UCE enrichment we made pools at equimolar concentrations containing 6-10

270 libraries. We adjusted pool concentration to 147 ng/µl using a vacuum centrifuge and

271 we used a total of 500 ng of DNA (3.4 µl of each pool) in each enrichment. We

272 performed enrichments using a custom RNA bait library developed for Hymenoptera

273 (Faircloth et al., 2015) and synthesized by MYcroarray (MYcroarray, Ann Arbor,

274 MI). The probe set includes 2,749 probes targeting 1,510 UCE loci. We enriched each

275 pool of samples following the manufacturer's protocol, except that for some pools, we

276 left streptavidin beads bound to enriched DNA during PCR (on-bead PCR). The

277 enrichment was performed at 65ºC for a period of 24 hours.

278

279 We verified enrichment success with qPCR by comparing amplification profiles of

280 unenriched to enriched pools for several UCE loci. After verification, we used qPCR

281 to measure the DNA concentration of each pool and we then combined all pools into

282 an equimolar final pool. At most we combined 110 samples together into the same

283 sequencing lane. To remove fragments that were either too large or too small for

284 sequencing, we size-selected pools from 300-800 bp using the Blue Pippin size

285 selection instrument (Sage Science, Beverly, MA). We mailed size-selected pools to

286 either the UCLA Neuroscience Genomics Core, Cornell's Institute of Biotechnology,

287 or the High Throughput Genomics Facility at the University of Utah, and we had the

288   samples sequenced as single lanes on an Illumina HiSeq 2500 (2x150 Rapid Run, or

289   2x125 v4 Run).

290

291   **Bioinformatics & DNA Matrix Preparation**

292

293   After sequencing, technicians at the sequencing centers demultiplexed and converted

294   the data from .bcl to .fastq format. Starting with the .fastq files, we performed all

295   initial bioinformatics steps, including read cleaning, assembly, and alignment, using

296   the software package PHYLUCE version 1.5 (Faircloth et al., 2012; Faircloth, 2015).

297   Raw reads were cleaned and trimmed using *illumiprocessor* and cleaned reads were

298   assembled *de novo* using the script *phyluce_assembly_assemblo_trinity*, which is a

299   wrapper around the assembly program Trinity v2013-02-25 (Grabherr et al., 2011).

300   We selected Trinity for read assembly because Faircloth et al. (2015) demonstrated

301   that it creates better assemblies with hymenopteran UCE data than other popular

302   assembly programs. After assembly, we mapped Trinity contigs to UCE loci using

303   *phyluce_assembly_match_contigs_to_probes*, with the *min-coverage* and *min-identity*

304   options set to 50 and 70, respectively. It should be noted that these less stringent

305   settings increased the average number of captured UCE loci by several hundred loci

306   as compared to the default settings in *phyluce*. Next, we used

307   *phyluce_assembly_get_match_counts* and

308   *phyluce_assembly_get_fastas_from_match_counts* to create a monolithic fasta file

309   containing all taxa and sequence data. During these steps we used the *incomplete-*

310   *matrix* flag to allow matrices to have missing data. We aligned all loci individually

311   using *phyluce_align_seqcap_align*, which runs the alignment program MAFFT

312   (Katoh et al., 2002). We used the *no-trim* and *incomplete-matrix* options during

313 alignment to prevent the data from being trimmed and to include loci with missing

314 data. We also adjusted the *min-length* and *proportion* options to 20 and 0.50,

315 respectively. After alignment, we used

316 *phyluce_align_get_gblocks_trimmed_alignments_from_untrimmed* to run the

317 trimming program GBLOCKS (Castresana, 2000; Talavera & Castresana, 2007) on

318 all aligned loci. We reduced the stringency of the default settings in GBLOCKS by

319 adjusting the b1, b2, b3, and b4 options to 0.5, 0.5, 12, and 7, respectively. These

320 settings were manually optimized by trial and error and visual inspection of

321 alignments.

322

323 **Phylogenetic Inference**

324

325 To reconstruct a robust phylogeny of the Stenammini we employed maximum

326 likelihood (ML), Bayesian (BI), and species tree (ST) methods. We started by

327 investigating the effect of missing data. To do this, we created several sets of filtered

328 alignments using the PHYLUCE script *phyluce_align_get_only_loci_with_min_taxa*.

329 This script removes loci that have fewer than a set percentange of the total number of

330 taxa. We filtered the alignments for 100, 99, 95, 90, 75, 50, and 25% taxa present and

331 we generated alignment stats for each locus set using the

332 *phyluce_align_get_align_summary_data* and *phyluce_align_get_informative_sites*

333 scripts. We then generated concatenated matrices for each locus set using the

334 *phyluce_align_format_nexus_files_for_raxml* script. With the exception of the 100

335 and 99% filtered matrices (these included very few loci), we analyzed all

336 concatenated matrices with RAxML v8.0.3 (Stamatakis, 2014), performing a rapid

337 bootstrap analysis (100 replicates) plus best tree search (option "–f a") using GTR+Γ

338   as the model of sequence evolution. The "best" filtering level was determined

339   subjectively by assessing matrix completeness, topology, and bootstrap scores. The

340   best filtering level was selected at 90% and this resulting set of alignments was used

341   for all subsequent analyses.

342

343   After filtering loci for missing data we carried out ML and BI analyses on the

344   concatenated matrix using the programs RAxML v8.0.3 (Stamatakis, 2014) and

345   ExaBayes v1.4.1 (Aberer et al., 2014), respectively. For both analyses we partitioned

346   the dataset using a development version of PartitionFinder (PF), which implements a

347   "kmeans" clustering algorithm to group similarly evolving sites together (Frandsen et

348   al. 2015). This approach, developed specifically for non-coding loci like UCEs,

349   identifies data subsets without user pre-partitioning. For the ML search we used the

350   rapid bootstrapping plus best-tree search algorithm ("-f a" option, 100 bootstrap

351   replicates) and we used GTR+Γ as the model of sequence evolution (for both best-tree

352   and bootstrap searches). For the BI search we executed two independent runs, each

353   with four coupled chains (one cold and three heated chains). We linked branch

354   lengths across partitions and we ran each partitioned search for one million

355   generations. We assessed burn-in, convergence among runs, and run performance by

356   examining parameter files with the program Tracer v1.6.0 (Rambaut et al., 2014). We

357   computed consensus trees using the *consense* utility, which comes as part of

358   ExaBayes.

359

360   To assess the possible influence of gene-tree conflict we performed species-tree

361   estimation using the summary method implemented in ASTRAL v4.8.0 (Mirarab et

362   al. 2014). To reduce error from loci with low information content we employed

363   weighted statistical binning, which bins loci together based on shared statistical

364   properties and then weights bins by the number of included loci (Bayzid et al., 2015).

365   To carry out the analysis, we first used RAxML to generate ML gene trees for all loci.

366   We then input the gene trees into the statistical binning pipeline using a support

367   threshold of 75 (recommend for data sets with < 1000 loci). This grouped genes into

368   168 bins, comprising 3 bins of 3 loci, 132 bins of 4 loci, and 33 bins of 5 loci. After

369   binning we concatenated the genes into supergenes and used RAxML to infer

370   supergene trees with bootstrap support (200 reps). We then input the resulting best

371   trees, weighted by gene number, and the bootstrap trees, into ASTRAL and conducted

372   a species tree analysis with 100 multi-locus bootstrap replicates (Seo, 2008).

373

374   **Divergence Dating**

375

376   To generate a time tree for the evolution of stenammine ants we estimated divergence

377   dates using the program BEAST v1.8 (Drummond et al., 2012). Due to computational

378   challenges arising from having both a large number of taxa and a large amount of

379   sequence data, we developed a two-part strategy to make the analyses feasible: (1) we

380   input a starting tree (all nodes constrained) and turned off tree-search operators and

381   (2) we input a subset of the sequence dataset rather than the entire concatenated

382   matrix. For the input tree we used the best tree generated from the partitioned

383   RAxML search and, for the data, we selected the 25 loci that had the highest gene tree

384   bootstrap scores. The selected loci were concatenated together and analyzed without

385   partitioning. We performed a total of four independent runs in BEAST, each for 100

386   million generations, sampling every one thousand generations. We also performed

387   one run in which the data were removed so that the MCMC search sampled from the

388   prior distribution only. For the clock model we selected uncorrelated lognormal, for

389   the substitution model we used GTR+Γ, and for the tree prior model we used birth-

390   death. For the ucld.mean prior we used an exponential distribution with mean 10.0.

391

392   To calibrate the analysis we used two secondary calibrations taken from Ward et al.

393   (2015). These were used rather than using fossil calibrations because most of the

394   fossils could not be placed within subgroups of Stenammini with high confidence. We

395   applied one secondary calibration to the root node (crown-group Myrmicinae) and

396   used a normal prior with mean 98.6 Ma and standard deviation 7 Ma. We applied the

397   other calibration to crown-group Stenammini and used a normal prior with mean 52.9

398   Ma and a standard deviation of 4 Ma.

399

400   To evaluate the performance of BEAST runs we inspected run parameters using

401   Tracer v1.6 (Rambaut et al. 2014). We looked for ESS values above 100 for all

402   parameters and for convergence among runs. After deciding on an appropriate burn-

403   in, we combined trees using *LogCombiner*, and generated a chronogram using

404   *TreeAnnotator* (both programs included with the BEAST package).

405

406   **Biogeographic Reconstruction**

407

408   We inferred the biogeographic history of Stenammini using the dispersal-extinction-

409   cladogenesis model (DEC; Ree & Smith, 2008) as implemented in the program RASP

410   (Yu et al., 2015). For input we used the consensus tree and 500 post-burnin trees from

411   the BEAST divergence dating analysis. Using the R package APE (Paradis et al.,

412   2004), we pruned all outgroup taxa from input trees, leaving only crown-group

413   Stenammini. We coded terminal taxa using the six classic biogeographic realms

414   (Olson et al., 2001; see Fig. 4c for coding): Nearctic (A), Neotropical (B), Palearctic

415   (C), Afrotropical (D), Indomalayan (E), and Australasian (F). Based on the

416   observation that most extant species occupy only one area, we set max areas to two

417   regions. We excluded several implausible ancestral areas (AD, AE, AF, BC, BD, BE,

418   BF, CF, CG, DE, DF) and reduced dispersal probabilities to 0 for several region pairs

419   (AD, AE, AF, BC, BE) and to 0.5 for several others (BD, BF, DF). Given the limited

420   amount of change in the position of continents during the timing of Stenammini

421   evolution (< 55 Ma, see results below), we used a single time slice for the analysis.

422   To take into account branch-length variation we performed a Bayes-DEC analysis in

423   RASP using 100 post-burnin trees randomly selected from the pool of 500. RASP

424   performs the DEC analysis on all 100 trees and plots the combined results on the

425   consensus tree.

426

427   **Habitat Reconstruction**

428

429   To gain further insight into niche evolution in Stenammini we inferred ancestral

430   habitats using the DEC model in RASP (i.e., the same approach used for

431   biogeographic reconstruction). All terminal taxa were coded as occupying one or a

432   combination of the following habitats (see Fig. 4c for coding): temperate wet (A),

433   temperate dry (B), tropical wet (C), or tropical dry (D). The implausible habitat

434   combinations AD and BC were excluded as possible ancestral states and dispersal

435   between these excluded habitat pairs was set to 0.5. For extratropical taxa we

436   considered nesting biology when coding species as being either wet or dry adapted.

437   Some *Veromessor* species, for example, occur in areas in the western USA that

438 receive periodic rainfall, but they nest in dry, open habitats. We coded these taxa as

439 B. Other species occur in the same general region as *Veromessor*, but are only active

440 in moist leaf litter (e.g., *Stenamma*). We coded these taxa as A. Several extratropical

441 taxa with uncertain or intermediate nesting habitats were coded as AB.

442

443 **Diversification Rates**

444

445 We investigated diversification dynamics in Stenammini using two main approaches.

446 First, we tested for significant shifts in diversification rate across the entire tree using

447 the R package TreePar (Stadler, 2011). TreePar is a ML-based program that allows

448 for non-constant diversification rates and incomplete taxon sampling. It fits a birth-

449 death model to dated trees and allows rates to change as a function of time. We ran

450 the program using the "bd.shifts.optim" function and used the dated consensus tree

451 from BEAST as the input tree (outgroups pruned). We set extant diversity at 22% to

452 account for incomplete species sampling (92/416 species sampled, including three

453 undescribed species) and we set the program to test for a maximum of five rate shifts

454 at 0.1 My intervals ranging from zero to 53 Ma. We selected the best-fitting model by

455 performing likelihood-ratio tests with significance assessed by P-values below 0.05.

456

457 After assessing tree-wide rate shifts, we tested for rate shifts among lineages using the

458 Bayesian program BAMM v2.5 (Bayesian Analysis of Macroevolutionary Mixtures;

459 Rabosky et al., 2013, 2014a; Rabosky, 2014; Shi & Rabosky, 2015) and the

460 accompanying R package BAMMtools (Rabosky et al., 2014b). BAMM is capable of

461 modeling complex diversification dynamics by exploring many models

462 simultaneously using reversible jump Markov Chain Monte Carlo (rjMCMC). A

463   major advantage over likelihood-based approaches is that this method allows one to

464   assess support for different rate-shift configurations using posterior probabilities and

465   Bayes Factors. It also allows for incomplete taxon sampling in a way that does not

466   require collapsing or pruning branches in the input tree.

467

468   For input into BAMM we used the BEAST consensus chronogram with outgroups

469   pruned. To account for non-random, incomplete taxon sampling we input a sampling

470   probability file, in which we assigned all terminals to clades roughly corresponding to

471   genera (*Aphaenogaster*, "Deromyrma", "Goniomma", *Messor*, *Novomessor*,

472   *Stenamma, Veromessor*; see Fig. 3) and we gave each clade a sampling probability

473   based on the number of species sampled and the number of extant species in that

474   clade (0.10, 0.46, 0.40, 0.05, 1.00, 0.45, and 0.89, respectively). To select appropriate

475   priors for the BAMM analysis, we used the "setBAMMpriors" function in

476   BAMMtools on the input time tree. Using the prior settings, we then ran the BAMM

477   analysis with four chains for 2,000,000 generations, sampling event data every 1,000

478   generations. After the analysis, we assessed burnin, run convergence, and ESS values

479   for all parameters using the R package CODA (Plummer et al., 2006). We then

480   explored the post-burnin output using BAMMtools and selected the best rate-shift

481   configuration by assessing posterior probabilities and Bayes Factors.

482

483   To visualize lineage accumulation through time, we used the APE package in R to

484   generate a lineage-through-time plot from the BEAST consensus tree and 500 post-

485   burnin trees

486

487   **RESULTS**

488

Diversity Gradient

490

We calculated latitudinal midpoints for all 413 extant species currently placed in the tribe Stenammini (Fig. 1). Using a cutoff for the tropics at 23.5ºN/S latitude, we found that 340 species are extratropical and only 73 species are tropical. The tribe ranges from roughly 30ºS to 50ºN and has an obvious diversity peak in the northern hemisphere between 35ºN to 40ºN latitude. The diversity distribution is strongly left-skewed, with richness dropping below ten species from 10ºN to 35ºS (binned at 5º intervals). This distribution is concordant with Stenammini having an inverse LDG, and thus being a contrarian clade.

499

UCE Phylogeny

501

Following sequencing, assembly, and the matching of probes to contigs, we recovered an average of 987 UCE contigs per sample, with a mean contig length of 909 bp and an average coverage score of 85X (see Appendix S3). We evaluated the results of filtering loci for taxon completeness and selected the 90% filtered matrix (*Filter90*) as the primary locus set for analysis (see Appendix S4 for filtering results). Following sequence alignment, the *Filter90* locus set included 702 loci and had an average locus length of 849 bp, resulting in a concatenated data set of 595,931 bp, of which 198,260 sites were informative. All sequences have been submitted to the NCBI Sequence Read Archive (upon acceptance) and the *Filter90* concatenated data set has been submitted to TreeBASE (upon acceptance)

512

513   The partitioned ML and BI analyses of the concatenated data set resulted in identical

514   topologies, with most nodes receiving maximum support (Fig. 2 and Appendix S5).

515   The few nodes with less than complete support were restricted to the shallower splits

516   in the tree. The ST analysis produced a mostly congruent tree (Appendix S5), with

517   one major difference involving the position of the genus *Messor* (discussed below).

518

519   We recovered the tribe Stenammini as monophyletic and comprising five major

520   clades: (1) the genus *Stenamma*, (2) the genera *Novomessor + Veromessor* (the

521   "Novomessor" clade), (3) a group of tropical "Aphaenogaster" (the "Deromyrma"

522   clade), (4) the genera *Goniomma* plus *Oxyopomyrmex* (the "Goniomma" clade), and

523   (5) the genus *Messor* plus all Holarctic members of *Aphaenogaster* (the

524   *"*Aphaenogaster" clade). The distributions of major groups are provided in Fig. 3.

525

526   The genus *Stenamma* was recovered as sister to the rest of the stenammine clades and

527   within *Stenamma,* the species *S. punctiventre*, a relict species form Morocco, was

528   found to be sister to all remaining species, which themselves separate into two major

529   clades that have previously been referred to as the "Holarctic" and "Middle

530   American" clades (Branstetter, 2012). These two clades are nearly geographically

531   isolated, overlapping only slightly in the southwestern USA.

532

533   Outside of *Stenamma*, the "Novomessor" clade was recovered as sister to all

534   remaining clades, and the genera *Novomessor* and *Veromessor* were each found to be

535   monophyletic. The "Deromyrma" clade was recovered as sister to the "Goniomma"

536   clade plus the "Aphaenogaster" clade. Unexpectedly, the "Deromyrma" clade was

537   found to include all tropical species of the genus *Aphaenogaster*, and these clustered

538 by region into New World and Old World clades. Within the "Goniomma" clade the

539 genus *Goniomma* was found to be paraphyletic with respect to *Oxyopomyrmex*.

540

541 In the "Aphaenogaster" clade we obtained conflicting results with respect to the

542 position of the genus *Messor*. In both the partitioned ML and BI analyses *Messor* is

543 monophyletic and sister to a monophyletic *Aphaenogaster*. However, in the ST

544 analysis the *Aphaenogaster* species *A. subterranean* and *A. leveillei* were found to be

545 sister to *Messor*, making *Aphaenogaster* paraphyletic. In the preliminary ML analyses

546 in which we assessed different levels of missing data, we also recovered

547 *Aphaenogaster* paraphyly (see Appendix S4). Uncertainty in *Aphaenogaster*

548 monophyly is also indicated in the partitioned ML and BI trees by low support and a

549 very short branch subtending the clade (Fig. 2).

550

551 **Historical Biogeography**

552

553 The following focuses on key nodes and combines the results of the BEAST

554 divergence dating analysis and the S-DEC biogeographic reconstruction. Dates are

555 presented as median ages and ancestral areas are presented as the most likely state,

556 except in cases in which different inferred areas have nearly the same probability.

557 Results are summarized in Fig. 4c, Table 1, and Appendix S6.

558

559 The tribe Stenammini evolved between 89-52 Ma (age between stem and crown

560 groups), with the crown group originating in the Holarctic region. Among the major

561 clades, most have an origin in the northern temperate zone. The genus *Stenamma*

562 originated in the Holarctic 41 Ma. The *"Goniomma"* and "Aphaenogaster" clades

563   both originated in the Palearctic region 15 Ma and 17 Ma, respectively.

564   Unexpectedly, the "Deromyrma" clade, which includes mostly tropical taxa (a few

565   species occur in temperate Australia), also was found to have a temperate origin, with

566   the ancestor inhabiting the Holarctic 41 Ma. The only major clade that may not have

567   had a temperate-only origin was the *"Novomessor"* clade. This group originated 22

568   Ma and was inferred to have either a Nearctic plus Neotropical origin (slightly higher

569   likelihood) or a Nearctic-only origin. Within the "Novomessor" clade, the DEC

570   model inferred a Nearctic plus Neotropical origin for *Novomessor* and a Nearctic-only

571   origin for *Veromessor*, 14 Ma and 11 Ma, respectively.

572

573   Across the tribe there were a total of six separate dispersal events out of the

574   extratropics and into the tropics. The ancestor of the Middle American clade of

575   *Stenamma* dispersed into the tropics 28-23 Ma. Depending on the reconstruction, the

576   ancestor of the "Novomessor" clade dispersed into the tropics between 50-22 Ma or

577   the ancestor of *Novomessor* dispersed into the tropics between 22-14 Ma. The genus

578   *Messor* dispersed into the Afrotropics more recently, 9-6 Ma. In the "Deromyrma"

579   clade we inferred three separate dispersals into the tropics, once into the Neotropics

580   41-13 Ma, once into Indomalaya 41-30 Ma, and once into the Afrotropics 12-11 Ma.

581

582   Dispersals out of the tropics and between the Nearctic and Palearctic regions also

583   occurred. We inferred three separate out-of-the-tropics dispersal events. The ancestor

584   of *S. huachucanum* back-dispersed from the Neotropics to the Nearctic between 11

585   Ma and the present. This species has a Neotropical plus Nearctic distribution,

586   reaching as far north as the sky islands of Arizona. In the genus *Messor*, dispersal into

587   the Afrotropics included dispersal into the arid subtropics of South Africa between 7-

588   2 Ma. Similarly, the Australian species *A. longiceps*, part of the "Deromyrma" clade,

589   occurs in tropical and extratropical Australia, likely having dispersed out of the

590   tropics between 15 Ma and the present. Dispersal from the Nearctic to the Palearctic

591   occurred once in the Holarctic clade of *Stenamma*, most likely between 10-6 Ma.

592   Finally, dispersal from the Palearctic into the Nearctic occurred in Holarctic

593   *Aphaenogaster* between 13-10 Ma.

594

595   **Niche Reconstruction**

596

597   We inferred ancestral habitats using the Bayes-DEC model in RASP (Fig. 4c, Table 1,

598   and Appendix S6). Concordant with the biogeographic results, for most major clades

599   we recovered temperate habitats for ancestral nodes. For crown-group Stenammini we

600   inferred a temperate wet plus temperate dry ancestral habitat. For the genus

601   *Stenamma* we inferred a temperate wet ancestor, with a shift into temperate wet plus

602   tropical wet habitats in the ancestor of the Holarctic plus Middle American clades.

603   The "Goniomma" clade had a temperate dry ancestor and the "Aphaenogaster" clade

604   had a temperate wet plus temperate dry ancestor. Both the "Novomessor" and

605   "Deromyrma" clades had temperate plus tropical ancestral habitats. In the

606   "Novomessor" clade we inferred the habitat to be temperate dry plus tropical dry. In

607   the "Deromyrma" clade we inferred the ancestor to have a temperate wet plus tropical

608   wet ancestral habitat, with most species shifting into a tropical wet habitat only.

609

610   **Diversification Dynamics**

611

612   Analysis with the program TreePar, which tests for diversification rate shifts across a

613   tree, found two rate shifts during stenammine evolution: one increase in net

614   diversification rate at 17.2 Ma during the Miocene (shift from 0.046 to 0.227 species

615   Myr^{-1}), and one decrease in rate at 1.9 Ma in the Pleistocene (shift from 0.227 to 001

616   species Myr^{-1}; Fig. 4ac & Appendix S7).

617

618   Complementing the TreePar results, diversification analysis with BAMM, which tests

619   for rate shifts among lineages, found high support for an increase in diversification

620   rate in the branch leading to the "Aphaenogaster" clade (Fig. 4c). The BAMM run

621   produced posterior probabilities for seven rate-shift models. Of these, the single rate-

622   shift model received the highest posterior probability (74%) and was favored by

623   Bayes Factor comparison as compared to the zero rate shift model (BF score of 2,666)

624   and all other shift models (see Appendix S7). The "Aphaenogaster" clade is dated to

625   17.2 Ma with the rate shift inferred to have occurred along the stem lineage several

626   million years prior to the origin of the crown group. Examining speciation rates

627   through time, the results show very similar, constant rates for all lineages except for

628   the "Aphaenogaster" clade (Fig. 4b, Table 2). The average speciation rate for the

629   entire tree was 0.174 species Myr^{-1} and the background rate ("Aphaenogaster" clade

630   excluded) was 0.123 species Myr^{-1}. The rate for just the "Aphaenogaster" clade was

631   0.363 species Myr^{-1}.

632

633   **DISCUSSION**

634

635   The current latitudinal diversity gradient, whereby species richness increases from

636   pole to equator, is the predominant diversity pattern found in most major organismal

637 lineages. An increasing number of groups, however, are known to exhibit non-

638 standard gradients. In this study we have added the ant tribe Stenammini, a large

639 taxon with over 400 species, to this growing list of contrarian clades. Our results

640 show that the tribe exhibits a strong inverse diversity gradient, with the majority of

641 taxa occurring in the northern temperate zone. Following this observation we used

642 phylogenomic techniques to establish a robust phylogeny for the tribe and we used

643 the phylogeny to evaluate alternative hypotheses that might explain the group's non-

644 standard diversity pattern.

645

646 **The latitudinal diversity gradient**

647

648 Using midpoint latitudes for all extant stenammine species, we demonstrated that the

649 tribe has a strong inverse diversity gradient, with the majority of species inhabiting

650 the northern temperate zone between 30-45ºN latitude (Fig. 1). Separating results by

651 clade (Fig. 1a) and biogeographic region (Fig. 1b), the diversity peak is mainly

652 attributable to *Aphaenogaster* and *Messor* species in the Palearctic. Could this pattern

653 be driven by a taxonomic or sampling bias? We strongly believe that the answer is no.

654 In recent years there has been extensive ant sampling by the authors and colleagues in

655 Central America, Africa, Madagascar, and Southeast Asia, and few additional tropical

656 morphospecies have been identified. Further, the genus *Stenamma,* which has the

657 highest tropical diversity among genera in the clade, was recently revised

658 (Branstetter, 2013) and we accounted for all new species in our analysis. In contrast to

659 tropical diversity, there have been several recent taxonomic revisions focusing on

660 Palearctic taxa and these studies have all added species to overall diversity

661 (Terayama, 2009; Boer, 2013; Borowiec & Salata, 2013, 2014; Kiran et al., 2013;

662   Salata & Borowiec, 2015). Furthermore, it is likely that many new Palearctic species

663   await discovery in poorly sampled regions, such as the southern Mediterranean and

664   Middle East.

665

666   A growing number of lineages from both the marine and terrestrial realms have been

667   identified as contrarian clades with extratropical peaks in species richness (Owen &

668   Owen, 1974; Dixon et al., 1987; Chown et al., 1998; Stephens & Wiens, 2003; Smith

669   et al., 2005; Krug et al., 2007; Pyron & Burbrink, 2009; Rivadeneira et al., 2015).

670   When considering these studies, it is important to distinguish between clade-based

671   and assemblage-based approaches. The clade-based studies have taken into account

672   species richness patterns for an entire monophyletic group. The assemblage-based

673   studies, however, investigated communities of species and are often spatially

674   restricted. Although the standard LDG might be considered an assemblage-based

675   phenomenon, we argue that identifying and studying contrarian clades helps to

676   explain diversity gradients broadly, especially when the clades of interest are diverse

677   and widespread. In our study we have taken a clade-based approach and have shown

678   that the ant tribe Stenammini is a diverse lineage that defies the standard LDG. Of the

679   available clade-based studies, in which a phylogenetic approach has been used to

680   examine an inverse LDG, ours represents the largest to date in terms of number of

681   species considered.

682

683   An interesting characteristic of the inverse gradient observed in Stenammini is its

684   skewed distribution. Even though the group extends into the southern temperate zone,

685   the diversity peak is only found in the northern hemisphere. This pattern of a northern

686   temperate species peak has been observed in lampropeltinine snakes (Pyron &

687   Burbrink, 2009), emydid turtles (Stephens & Wiens, 2003), and several clades of

688   hylid frogs (Smith et al., 2005). Salamanders also show this pattern at the family

689   level, but not at the species level (Wiens, 2007). In contrast, marine bivalves (Krug et

690   al., 2007) and aphids (Dixon et al., 1987) have diversity peaks in both the northern

691   and southern hemispheres. Currently there are no clade-based studies that have shown

692   a skewed distribution in which diversity peaks in the southern temperate zone. A

693   number of studies have shown an inverse diversity gradient along the coast of South

694   America, but these studies have focused on species assemblages rather than clades

695   (Rivadeneira et al., 2011). Other groups with temperate richness peaks but uncertain

696   symmetry include pelagic seabirds (Chown et al., 1998) and ichneumonid wasps

697   (Owen & Owen, 1974). As discussed below this skewed distribution of Stenammini is

698   likely due its origin in the northern hemisphere.

699

700   **Evolution of Stenammini**

701

702   Crown-group Stenammini originated in the Holarctic during the early Eocene

703   approximately 53 Ma. This time period corresponds to the Eocene Climatic Optimum

704   (ECO) when temperatures were on average 5-6ºC warmer than today (Zachos et al.,

705   2001) and broad-leaved evergreen forest and paratropical rainforest were greatly

706   expanded (Graham, 1993, 2011). Fossil records indicate that broad-leaved, evergreen

707   forest extended above 70ºN latitude (Eberle & Greenwood, 2012; Harrington et al.,

708   2012) and that animals with present-day tropical affinities, such as the Arctic tapir,

709   inhabited these forests (Eberle & Greenwood, 2012). It is also known that the

710   vegetation in North America and Eurasia was more homogeneous during this time,

711   likely due to the lack of polar glaciation and the existence of two major land bridges,

712   the Bering Land Bridge (75ºN) and the North Atlantic Land Bridge (45-65ºN) (Wing,

713   1987). Stenammini, therefore, originated in the Holarctic at a time when wet forest

714   habitat dominated the northern hemisphere and significant connections between

715   northern continents existed, facilitating dispersal. Our inferred ancestral habitat for

716   the tribe of temperate wet and temperate dry is in line with the idea that the ancestral

717   stenammine species could have existed throughout the Holarctic in both the dominant

718   forest habitat and the more limited deciduous and dry habitats.

719

720   After the ECO there was a gradual decrease in global temperature culminating in a

721   sharp decrease 35 Ma at the Eocene-Oligocene boundary. During the cooling, the

722   evergreen forests retracted from their northern maxima, and more seasonal habitats,

723   including deciduous forest, expanded (Wing, 1987; Graham, 2011). This period of

724   time is important because many modern plant and animal lineages originated (Wing,

725   1987; Pellmyr & Leebens-Mack, 1999; Bininda-emonds et al., 2007; Jaramillo et al.,

726   2010). For plants the homogeneous nature of the vegetation between North American

727   and Eurasia began to disappear, suggesting that dispersal via the northern land bridges

728   became increasingly less likely, especially for species adapted to warm, wet

729   environments. This observation that wet-adapted species were once widespread across

730   Eurasia, but then had to retract into tropical refugia has become known as the

731   Boreotropics hypothesis and is commonly proposed in phytogeography to explain

732   taxa with disjunct distributions between the Old World and New World tropics

733   (Wolfe, 1975; Tiffney, Bruce, 1985; Lavin & Luckow, 1993; Donoghue, 2008). We

734   believe this scenario is important in considering the evolution of Stenammini,

735   especially for the "Deromyrma" clade.

736

737   The *"Deromyrma"* clade can be aptly described as a tropical group even though a few

738   species extend into the Australian temperate zone. Our phylogenetic results show that

739   the clade originated ~41 Ma and bifurcated into New and Old World lineages.

740   Contrary to expectations, we found that the clade originated in the Holarctic and

741   dispersed into the tropics three times, once into Mesoamerica, once into Indomalaya,

742   and once into the Afrotropics. Our biogeographic reconstruction is completely

743   concordant with the Boreotropics hypothesis. The ancestor of the "Deromyrma" clade

744   was widespread and adapted to wet evergreen forest habitat. When the wet forest

745   contracted and no longer extended across the northern land bridges, "Deromyrma"

746   separated vicariantly into the New and Old World lineages. Both of these lineages

747   then followed the retraction of wet forest into the tropics, where they have persisted to

748   the present. This scenario is concordant with the fossil record, which includes a

749   species from Dominican Amber (*Aphaenogaster amphiocenica*) that has been

750   suggested to be closely related to tropical *Aphaenogaster* (De Andrade, 1995)

751

752   In the Old World tropics the "Deromyrma" clade has penetrated into Indomalaya,

753   Australasia, and Madagascar (Afrotropics). How the clade arrived in Madagascar is

754   interesting to consider, since it is not known from mainland Africa. Our

755   biogeographic reconstruction suggests that the clade dispersed into the Afrotropics

756   from the Palearctic rather than from Indomalaya or Australasia. This scenario

757   suggests dispersal through Africa to reach Madagascar with later extinction from the

758   mainland. A "through-Africa" hypothesis is supported by the fact that most extant

759   Malagasy taxa have African origins (Yoder & Nowak, 2006) and rainforest was once

760   more extensive in Africa during the Eocene (Burgess et al., 1998; Couvreur et al.,

761   2008).

762

763 Global cooling explains another intriguing diversification event within the

764 Stenammini. The ant genus *Stenamma* includes three clades, the relict Palearctic

765 taxon *S. punctiventre*, a Holarctic clade, and a Middle American clade. The species *S.*

766 *punctiventre* is included in a phylogeny for the first time here. Unexpectedly, the

767 species was placed as sister to all remaining *Stenamma,* pushing the age of the crown

768 group back to 41 Ma. Previous work inferred the origin of *Stenamma* to be Nearctic

769 (Branstetter, 2012), but with *S. punctiventre* included, we inferred the origin of the

770 genus to be Holarctic. The two major clades in the genus each contain about 40

771 species, with the Holarctic clade including a mix of Nearctic and Palearctic lineages

772 and the Middle American clade including predominately Central American species,

773 with only a couple of species reaching northern Mexico/southern U.S.A. and a few

774 reaching northern South America. The timing of the split for these two clades is ~28

775 Ma. This date overlaps closely with the sharp cooling event at the Eocene-Oligocene

776 boundary, which caused the mesic forests that once stretched between North and

777 Central America to become fragmented due to aridification in the southwestern USA

778 and northern Mexico (Wing, 1987). Given that *Stenamma* is generally associated with

779 wet forest leaf litter, this aridification event is likely what caused the nearly complete

780 split between northern and southern clades. More recently, the Middle American

781 clade back-dispersed to the Nearctic via montane sky islands (e.g., *Stenamma*

782 *huachucanum*).

783

784 The strong association of Stenammini with the northern temperate zone is further

785 exemplified by the *"Goniomma"* and "Aphaenogaster" clades having ancestral areas

786 in the Palearctic region. The "Goniomma" clade originated ~15 Ma and is completely

787   restricted to the Mediterranean region. The "Aphaenogaster" clade is about the same

788   age (17 Ma), but has spread more widely across the globe. It is distributed across the

789   Holarctic and with the genus *Messor* has penetrated into arid regions in Africa,

790   extending all the way down into South Africa.

791

792   The only major clade that does not have a completely north-temperate origin is the

793   "Novomessor" clade. This group is arid-adapted and likely evolved in the Nearctic

794   plus Neotropics or just the Nearctic with later dispersal into the Neotropics. The age

795   of the clade is 22 Ma and it is split into the two monophyletic genera *Novomessor* and

796   *Veromessor*. The former is distributed more southerly into Mexico, whereas the latter

797   is more diverse in the western USA. It is possible that these two genera separated into

798   northern and southern lineages during periods of increased aridification, similar to the

799   pattern observed in *Stenamma*.

800

801   The results of the diversification analysis provide a compelling scenario for how

802   Stenammini reached its current species-richness levels. Considering the across-tree

803   analysis, we inferred an increase in diversification rate at 17.2 Ma and a slowdown at

804   1.9 Ma (Fig. 4a-c). This time period includes the origin of all of the more diverse

805   clades in the tribe and it corresponds to the Mid-Miocene Climatic Optimum

806   (MMCO) and a major decrease in global temperature that has continued to the

807   present. Thus, while most higher-level diversification in the tribe is linked to global

808   cooling after the ECO, most species-level diversity is correlated with cooling

809   following the MMCO. It is very likely that the fragmentation of habitats caused by

810   increased aridification during this time contributed to allopatric diversification in the

811   tribe. The other important result is that among lineages, there was a significant

812   increase in diversification rate leading to the "Aphaenogaster" clade. The importance

813   of this rate shift to the overall diversification dynamics is obvious when the

814   "Aphaenogaster" clade is excluded and only the background rate is examined (Fig.

815   4b, black line). This result suggests that most stenammine lineages have been

816   evolving at a constant rate, but that the "Aphaenogaster" clade experienced a

817   significant rate increase starting just prior to 17.2 Ma.

818

819   Why did the "Aphaenogaster" clade diversify significantly faster than the other

820   lineages? We believe the answer can be linked to the group's ecological diversity and

821   its ties to the Mediterranean region. The clade includes two major genera, *Messor* and

822   *Aphaenogaster.* The former is a specialist seed-harvester that is well adapted to desert

823   and grassland habitats. These adaptations include size polymorphism, with the

824   soldiers having large, muscular heads for eating seeds, and long beard-like hairs

825   underneath the head, which are used for transporting excavated sand. *Messor* is

826   currently widespread, occurring throughout the Palearctic and into arid Africa. The

827   genus *Aphaenogaster* is more varied in its habits, but tends to be a medium-sized

828   epigeic ant that is omnivorous. It does well in temperate forests and seasonally dry

829   areas around the Mediterranean. Given the ability of both genera to do well in

830   seasonally dry areas, increasing aridification over the last 20 Ma may have promoted

831   diversification by fragmenting forested habitats and expanding arid environments.

832

833   The overall pattern of evolution in Stenammini suggests that it has been most

834   successful in temperate habitats. All the major clades evolved in one or both of the

835   Holarctic regions and the majority of the species diversity is found there. Even though

836   the clade has dispersed to the tropics at least six times, the majority of those tropical

837   lineages have failed to diversify greatly. The only exception to this is the ant genus

838   *Stenamma*, which includes a lineage that has radiated into over 40 species in Central

839   America. This lineage, however, does not exhibit a significantly higher diversification

840   rate as compared to its Holarctic sister clade and it shows a clear connection to its

841   temperate past: it is a montane specialist with greatest diversity and abundance in wet

842   forest above 1,000 m. This pattern contrasts with ants generally, which show greater

843   diversity and abundance in the tropical lowlands.

844

845   **Evaluating alternative LDG hypotheses**

846

847   Using our results we can differentiate among several competing hypotheses that

848   might explain the inverse latitudinal gradient exhibited by Stenammini. These

849   hypotheses are the time-for-speciation/center-of-origin (TFS/COO) hypothesis

850   (Schluter, 1993; Wiens & Donoghue, 2004; Stevens, 2006), the niche conservatism

851   hypothesis (Wiens & Donoghue, 2004; Wiens & Graham, 2005), and the

852   diversification rate hypothesis (Rohde, 1992; Cardillo et al., 2005; Weir & Schluter,

853   2007). Given that Stenammini is most diverse in the northern temperate zone, the

854   TFS/COO would predict that the clade originated in this region and thus has had more

855   time to diversify there. This prediction is supported. The tribe originated in the

856   Holarctic, as did most of the major clades. It is also supported by the fact that the

857   Middle American and Holarctic clades of *Stenamma* have nearly the same number of

858   species. These clades are the same age and thus should have about the same number

859   of species under the TFS/COO.

860

861   The niche conservatism hypothesis predicts that niche evolution is rare and that the

862   niche with the most species will be the ancestral niche. For Stenammini, this

863   hypothesis is partly supported. We inferred the ancestral habitat to be temperate wet

864   and temperate dry. Moreover, the majority of extant species inhabit the ancestral

865   niche. Evidence against niche conservatism is the fact that the tribe dispersed into the

866   tropics six separate times, which suggests that niche evolution is not rare in this

867   lineage. However, there are two major considerations when examining these shifts.

868   First, none of these shifts have been followed by an increase in diversification rate,

869   which has left most of these tropical clades depauperate. Second, the ecology of some

870   of these lineages belies their tropical distribution. For example, the Middle American

871   clade of *Stenamma* has radiated in montane Mesoamerica, likely because of its

872   ancestral adaptation to cool environments. Thus, while the tribe has shifted into the

873   tropics multiple times, they have not been very successful at radiating into the niches

874   occupied by most tropical ants, possibly due to competition.

875

876   Lastly, the diversification rate hypothesis predicts that differences in species richness

877   are due to differences in speciation and extinction rates among clades. In the context

878   of the standard LDG, the idea is that tropical clades will have higher speciation or

879   lower extinction rates compared to temperate clades. However, in the case of an

880   inverse LDG the opposite should be true. Thus, for Stenammini, we expect to see a

881   higher diversification rate in temperate lineages. Overall this prediction is confirmed.

882   Specifically, we found a significant increase in the diversification rate of the

883   "Aphaenogaster" clade, a lineage with mostly temperate species. Moreover, the

884   average speciation rate for temperate species was significantly higher than for tropical

885   species. It should be noted, however, that with the "Aphaenogaster" clade excluded,

886   the diversification rates among the remaining lineages, tropical or temperate, were

887   similar.

888

889   To summarize, the predictions made by all three hypotheses are supported by our

890   results. Stenammini has had more time to diversify in the temperate zone, it has

891   maintained its ancestral niche as the most common niche, and it has exhibited a

892   higher diversification rate among temperate species. Thus, all three proposed factors

893   have contributed to the inverse diversity gradient that we see today in the

894   Stenammini.

895

896   **ACKNOWLEDGMENTS**

897

914

915   **REFERENCES**

916

917   Aberer A.J., Kobert K., & Stamatakis A. (2014) ExaBayes: massively parallel

918   Bayesian tree inference for the whole-genome era. *Molecular Biology and*

919   *Evolution*, **31**, 2553–2556.

920   De Andrade M.L. (1995) The ant genus *Aphaenogaster* in Dominican and Mexican

921   amber (Amber Collection Stuttgart: Hymenoptera, Formicidae. IX: Pheidolini).

922   *Stuttgarter Beiträge zur Naturkunde. Serie B (Geologie und Paläontologie)*, **223**,

923   1–11.

924   Bayzid M.S., Mirarab S., Boussau B., & Warnow T. (2015) Weighted statistical

925   binning: enabling statistically consistent genome-scale phylogenetic analyses.

926   *PLoS ONE*, **10**, e0129183.

927   Bininda-emonds O.R.P., Cardillo M., Jones K.E., Macphee R.D.E., Beck R.M.. D.,

928   Grenyer R., Price S.A., Vos R.A., Gittleman J.L., & Purvis A. (2007) The

929   delayed rise of present-day mammals. *Nature*, **446**, 507–512.

930   Boer P. (2013) Revision of the European ants of the *Aphaenogaster testaceopilosa*-

931   group (Hymenoptera: Formicidae). *Tijdschrift voor Entomologie*, **156**, 57–93.

932   Bolton B. (1982) Afrotropical species of the myrmicine ant genera *Cardiocondyla*,

933   *Leptothorax*, *Melissotarsus*, *Messor* and *Cataulacus* (Formicidae). *Bulletin of the*

934   *Brittish Museum of Natural History (Entomology)*, **45**, 307–370.

935   Bolton B. (2015) An online catalog of the ants of the world. Available at

936   www.http://antcat.org. [Date Accessed: 2015-12-01]

937   Borowiec L. & Salata S. (2013) Ants of Greece – additions and corrections

938   (Hymenoptera: Formicidae). *Genus*, **24**, 335–401.

939   Borowiec L. & Salata S. (2014) Review of Mediterranean members of the

940   *Aphaenogaster cecconii* group (Hymenoptera: Formicidae), with description of

941   four new species. *Zootaxa*, **3861(1)**, 40–60.

942   Brady S.G., Schultz T.R., Fisher B.L., & Ward P.S. (2006) Evaluating alternative

943   hypotheses for the early evolution and diversification of ants. *Proceedings of the*

944   *National Academy of Sciences*, **103**, 18172–18177.

945   Branstetter M.G. (2009) The ant genus *Stenamma* Westwood (Hymenoptera:

946   Formicidae) redefined, with a description of a new genus *Propodilobus*.

947   *Zootaxa*, **2221**, 41–57.

948   Branstetter M.G. (2012) Origin and diversification of the cryptic ant genus *Stenamma*

949   Westwood (Hymenoptera: Formicidae), inferred from multilocus molecular data,

950   biogeography and natural history. *Systematic Entomology*, **37**, 478–496.

951   Branstetter M.G. (2013) Revision of the Middle American clade of the ant genus

952   *Stenamma* Westwood (Hymenoptera, Formicidae, Myrmicinae). *ZooKeys*, **295**,

953   1–277.

954   Brown J.H. (2014) Why are there so many species in the tropics? *Journal of*

955   *Biogeography*, **41**, 8–22.

956   Burgess N.D., Clarke G.P., & Rodgers W.A. (1998) Coastal forests of eastern Africa:

957   status, endemism patterns and their potential causes. *Biological Journal of the*

958   *Linnean Society*, **64**, 337–367.

959   Cardillo M., Orme C.D.L., & Owens I.P.F. (2005) Testing for latitudinal bias in

960   diversification rates: An example using new world birds. *Ecology*, **86**, 2278–

961   2287.

962   Carpenter F.M. (1930) The fossil ants of North America. *Bulletin of the Museum of*

963   *Comparative Zoology*, **70**, 1–66.

964   Castresana J. (2000) Selection of conserved blocks from multiple alignments for their

965   use in phylogenetic analysis. *Molecular Biology and Evolution*, **17**, 540–552.

966   Chown S.L., Gaston K.J., & Williams P.H. (1998) Global patterns in species richness

967   of pelagic seabirds: the Procellariiformes. *Ecography*, **21**, 342–350.

968   Couvreur T.L.P., Chatrou L.W., Sosef M.S.M., & Richardson J.E. (2008) Molecular

969   phylogenetics reveal multiple tertiary vicariance origins of the African rain forest

970   trees. *BMC biology*, **6**, 54.

971   Demarco B.B. & Cognato A.I. (2015) Phylogenetic analysis of *Aphaenogaster*

972   supports the resurrection of *Novomessor* (Hymenoptera: Formicidae). *Annals of*

973   *the Entomological Society of America*, **108**, 201–210.

974   Dixon A.F.G., Kindlmann P., Leps J., & Holman J. (1987) Why there are so few

975   species of aphids, especially in the tropics. *The American Naturalist*, **129**, 580–

976   592.

977   Donoghue M.J. (2008) A phylogenetic perspective on the distribution of plant

978   diversity. *Proceedings of the National Academy of Sciences*, **105**, 11549–11555.

979   Drummond A.J., Suchard M.A., Xie D., & Rambaut A. (2012) Bayesian

980   phylogenetics with BEAUti and the BEAST 1.7. *Molecular Biology and*

981   *Evolution*, **29**, 1969–1973.

982   Eberle J.J. & Greenwood D.R. (2012) Life at the top of the greenhouse Eocene world:

983   a review of the Eocene flora and vertebrate fauna from Canada's High Arctic.

984   *Geological Society of America Bulletin*, **124**, 3–23.

985   Faircloth B.C. (2015) PHYLUCE is a software package for the analysis of conserved

986   genomic loci. *Bioinformatics*, **Advance Access**, 1–3.

987   Faircloth B.C., Branstetter M.G., White N.D., & Brady S.G. (2015) Target

988   enrichment of ultraconserved elements from arthropods provides a genomic

989   perspective on relationships among Hymenoptera. *Molecular Ecology*

990   *Resources*, **15**, 489–501.

991   Faircloth B.C. & Glenn T.C. (2012) Not all sequence tags are created equal:

992   designing and validating sequence identification tags robust to indels. *PloS ONE*,

993   **7**, e42543.

994   Faircloth B.C., McCormack J.E., Crawford N.G., Harvey M.G., Brumfield R.T., &

995   Glenn T.C. (2012) Ultraconserved elements anchor thousands of genetic markers

996   spanning multiple evolutionary timescales. *Systematic Biology*, **61**, 1–10.

997   Field R., Hawkins B.A., Cornell H. V., Currie D.J., Diniz-Filho J.A.F., Guégan J.-F.,

998   Kaufman D.M., Kerr J.T., Mittelbach G.G., Oberdorff T., O'Brien E.M., &

999   Turner J.R.G. (2009) Spatial species-richness gradients across scales: a meta-

1000   analysis. *Journal of Biogeography*, **36**, 132–147.

1001   Frandsen P.B., Calcott B., Mayer C., & Lanfear R. (2015) Automatic selection of

1002   partitioning schemes for phylogenetic analyses using iterative k-means clustering

1003   of site rates. *BMC Evolutionary Biology*, **15**, 1–17.

1004   Grabherr M.G., Haas B.J., Yassour M., Levin J.Z., Thompson D.A., Amit I., Adiconis

1005   X., Fan L., Raychowdhury R., Zeng Q., Chen Z., Mauceli E., Hacohen N.,

1006   Gnirke A., Rhind N., di Palma F., Birren B.W., Nusbaum C., Lindblad-Toh K.,

1007   Friedman N., & Regev A. (2011) Full-length transcriptome assembly from

1008   RNA-Seq data without a reference genome. *Nature Biotechnology*, **29**, 644–52.

1009   Graham A. (1993) History of the vegetation: Cretaceous (Maastichtian)-Tertiary.

1010   *Flora of North America North of Mexico, Vol. 1* (ed. by F. of N.A.E. Committe),

1011   pp. 57–70. Oxford University Press, New York.

1012   Graham A. (2011) The age and diversification of terrestrial new world ecosystems

1013   through Cretaceous and Cenozoic time. *American Journal of Botany*, **98**, 336–

1014   351.

1015   Guénard B., Economo E.P., Weiser M.D., Gomez K., & Narula N. (2015)

1016   antmaps.org. Available at: http://antmaps.org/about.html. [Date Accessed: 2015-

1017   12-01].

1018   Harrington G.J., Eberle J., Le-Page B.A., Dawson M., & Hutchison J.H. (2012) Arctic

1019   plant diversity in the Early Eocene greenhouse. *Proceedings of the Royal Society*

1020   *B*, **279**, 1515–1521.

1021   Hawkins B.A. (2001) Ecology's oldest pattern? *Trends in Ecology & Evolution*, **16**,

1022   470.

1023   Hillebrand H. (2004) On the generality of the latitudinal diversity gradient. *The*

1024   *American Naturalist*, **163**, 192–211.

1025   Hölldobler B. & Wilson E.O. (1990) *The Ants.* Belknap Press, Cambridge, MA.

1026   Jablonski D., Kaustuv R., & Valentine J.W. (2006) Out of the tropics: evolutionary

1027   dynamics of the latitudinal diversity gradient. *Science*, **314**, 102–106.

1028   Jaramillo C., Ochoa D., Contreras L., Pagani M., Romero M., Quiroz L., Rodriguez

1029   G., Rueda M.J., de la Parra F., Morón S., Green W., Bayona G., Montes C.,

1030   Quintero O., Ramirez R., Mora G., Schouten S., Bermudez H., Navarrete R.,

1031   Parra F., Alvarán M., Osorno J., Crowley J., Valencia V., & Vervoort J. (2010)

1032   Effects of rapid global warming at the Paleocene-Eocene boundary on

1033   Neotropical vegetation. *Science*, **330**, 957–962.

1034   Johnson R.A. (2001) Biogeography and community structure of North American

1035   seed-harvester ants. *Annual Review of Entomology*, **46**, 1–29.

1036 Kaspari M., Yuan M., & Alonso L. (2003) Spatial grain and the causes of regional

1037   diversity gradients in ants. *The American Naturalist*, **161**, 459–477.

1038 Katoh K., Misawa K., Kuma K., & Miyata T. (2002) MAFFT: a novel method for

1039   rapid multiple sequence alignment based on fast Fourier transform. *Nucleic*

1040   *Acids Research*, **30**, 3059–66.

1041 Kiran K., Alipanah H., & Paknia O. (2013) A new species of the ant genus

1042   *Aphaenogaster* Mayr (Hymenoptera: Formicidae) from Iran. *Asian*

1043   *Myrmecology*, **5**, 45–51.

1044 Krug A.Z., Jablonski D., & Valentine J.W. (2007) Contrarian clade confirms the

1045   ubiquity of spatial origination patterns in the production of latitudinal diversity

1046   gradients. *Proceedings of the National Academy of Sciences*, **104**, 18129–18134.

1047 Lavin M. & Luckow M. (1993) Origins and relationships of tropical North America

1048   in the context of the boreotropics hypothesis. *American Journal of Botany*, **80**,

1049   1–14.

1050 Mannion P.D., Upchurch P., Benson R.B.J., & Goswami A. (2013) The latitudinal

1051   biodiversity gradient through deep time. *Trends in Ecology & Evolution*, **29**, 42–

1052   50.

1053 Mirarab S., Reaz R., Bayzid M.S., Zimmermann T., Swenson M.S., & Warnow T.

1054   (2014) ASTRAL: genome-scale coalescent-based species tree estimation.

1055   *Bioinformatics*, **30**, i541–i548.

1056 Moreau C.S. & Bell C.D. (2013) Testing the museum versus cradle tropical biological

1057   diversity hypothesis: phylogeny, diversification, and ancestral biogeographic

1058   range evolution of the ants. *Evolution*, **67**, 2240–2257.

1059 Olson D.M., Dinerstein E., Wikramanayake E.D., Burgess N.D., Powell G.V.N.,

1060   Underwood E.C., D'amico J.A., Itoua I., Strand H.E., Morrison J.C., Loucks

1061   C.J., Allnutt T.F., Ricketts T.H., Kura Y., Lamoreux J.F., Wettengel W.W.,

1062   Hedao P., & Kassem K.R. (2001) Terrestrial ecoregions of the world: a new map

1063   of life on Earth. *BioScience*, **51**, 933–938.

1064   Owen D.F. & Owen J. (1974) Species diversity in temperate and tropical

1065   Ichneumonidae. *Nature*, **249**, 583–584.

1066   Paradis E., Claude J., & Strimmer K. (2004) APE: Analyses of Phylogenetics and

1067   Evolution in R language. *Bioinformatics*, **20**, 289–290.

1068   Pellmyr O. & Leebens-Mack J. (1999) Forty million years of mutualism: evidence for

1069   Eocene origin of the yucca-yucca moth association. *Proceedings of the National*

1070   *Academy of Sciences*, **96**, 9178–9183.

1071   Pianka E.R. (1966) Latitudinal gradients in species diversity: a review of concepts.

1072   *The American Naturalist*, **100**, 33–46.

1073   Plummer M., Best N., Cowles K., & Vines K. (2006) CODA: Convergence Diagnosis

1074   and Output Analysis for MCMC. *R News*, **6**, 7–11.

1075   Pyron R.A. & Burbrink F.T. (2009) Can the tropical conservatism hypothesis explain

1076   temperate species richness patterns? An inverse latitudinal biodiversity gradient

1077   in the New World snake tribe Lampropeltini. *Global Ecology and Biogeography*,

1078   **18**, 406–415.

1079   Rabosky D.L. (2014) Automatic detection of key innovations, rate shifts, and

1080   diversity-dependence on phylogenetic trees. *PloS one*, **9**, e89543.

1081   Rabosky D.L., Donnellan S.C., Grundler M., & Lovette I.J. (2014a) Analysis and

1082   visualization of complex macroevolutionary dynamics: an example from

1083   Australian scincid lizards. *Systematic Biology*, **63**, 610–627.

1084   Rabosky D.L., Grundler M., Anderson C., Title P., Shi J.J., Brown J.W., Huang H., &

1085   Larson J.G. (2014b) BAMMtools : an R package for the analysis of evolutionary

1086   dynamics on phylogenetic trees. *Methods in Ecology and Evolution*, **5**, 701–707.

1087 Rabosky D.L., Santini F., Eastman J., Smith S.A., Sidlauskas B., Chang J., & Alfaro

1088   M.E. (2013) Rates of speciation and morphological evolution are correlated

1089   across the largest vertebrate radiation. *Nature Communications*, **4**, 1958.

1090 Rambaut A., Suchard M.A., Xie D., & Drummond A.J. (2014) Tracer v1.6, Available

1091   from http://beast.bio.ed.ac.uk/Tracer.

1092 Ree R.H. & Smith S.A. (2008) Maximum likelihood inference of geographic range

1093   evolution by dispersal, local extinction, and cladogenesis. *Systematic Biology*,

1094   **57**, 4–14.

1095 Rivadeneira M.M., Alballay A.H., Villafaña J.A., Raimondi P.T., Blanchette C.A., &

1096   Fenberg P.B. (2015) Geographic patterns of diversification and the latitudinal

1097   gradient of richness of rocky intertidal gastropods: the "into the tropical

1098   museum" hypothesis. *Global Ecology and Biogeography*, **24**, 1149–1158.

1099 Rivadeneira M.M., Thiel M., González E.R., & Haye P.A. (2011) An inverse

1100   latitudinal gradient of diversity of peracarid crustaceans along the Pacific Coast

1101   of South America: out of the deep south. *Global Ecology and Biogeography*, **20**,

1102   437–448.

1103 Rohde K. (1992) Latitudinal gradients in species-diversity: the search for the primary

1104   cause. *Oikos*, **65**, 514–527.

1105 Salata S. & Borowiec L. (2015) A taxonomic revision of the genus *Oxyopomyrmex*

1106   André, 1881 (Hymenoptera: Formicidae). **4025**, 1–66.

1107 Schluter D. (1993) *Species diversity: historical and geographical perspectives.*

1108   University of Chicago Press, Chicago.

1109 Seo T.K. (2008) Calculating bootstrap probabilities of phylogeny using multilocus

1110   sequence data. *Molecular Biology and Evolution*, **25**, 960–971.

1111   Shi J.J. & Rabosky D.L. (2015) Speciation dynamics during the global radiation of

1112   extant bats. *Evolution*, **69**, 1528–1545.

1113   Smith S.A., Stephens P.R., & Wiens J.J. (2005) Replicate patterns of species richness,

1114   historical biogeography, and phylogeny in Holarctic treefrogs. *Evolution*, **59**,

1115   2433–2450.

1116   Stadler T. (2011) Mammalian phylogeny reveals recent diversification rate shifts.

1117   *Proceedings of the National Academy of Sciences*, **108**, 6187–6192.

1118   Stamatakis A. (2014) RAxML version 8: A tool for phylogenetic analysis and post-

1119   analysis of large phylogenies. *Bioinformatics*, **30**, 1312–1313.

1120   Stephens P.R. & Wiens J.J. (2003) Explaining species richness from continents to

1121   communities: the time-for-speciation effect in emydid turtles. *The American*

1122   *Naturalist*, **161**, 112–128.

1123   Stevens R.D. (2006) Historical processes enhance patterns of diversity along

1124   latitudinal gradients. *Proceedings of the Royal Society B*, **273**, 2283–2289.

1125   Talavera G. & Castresana J. (2007) Improvement of phylogenies after removing

1126   divergent and ambiguously aligned blocks from protein sequence alignments.

1127   *Systematic Biology*, **56**, 564–577.

1128   R Core Team (2015) R: A language and environment for statistical computing. R

1129   Foundation for Statistical Computing, Vienna, Austria.

1130   Terayama M. (2009) A synopsis of the family Formicidae of Taiwan (Insecta,

1131   Hymenoptera). *Research Bulletin of Kanto Gakuen University. Liberal Arts.*, **17**,

1132   81–266.

1133   Tiffney, Bruce H. (1985) The Eocene North Atlantic land bridge: its importance in

1134   Tertiary and modern phytogeography of the Northern Hemisphere. *Journal of*

1135   *the Arnold Arboretum*, **66**, 243 – 273.

1136 Ward P.S., Brady S.G., Fisher B.L., & Schultz T.R. (2015) The evolution of

1137   myrmicine ants: phylogeny and biogeography of a hyperdiverse ant clade

1138   (Hymenoptera: Formicidae). *Systematic Entomology*, **40**, 61–81.

1139 Weir J.T. & Schluter D. (2007) The latitudinal gradient in recent speciation and

1140   extinction rates of birds and mammals. *Science*, **315**, 1574–1576.

1141 Wheeler W.M. (1915) The ants of the Baltic Amber. *Schriften der Physikalisch-*

1142   *Ökonomischen Gesellschaft zu Königsberg*, **55**, 1–142.

1143 Whitford W.G., Depree E., & Johnson P. (1980) Foraging ecology of two Chihuahuan

1144   desert ant species: *Novomessor cockerelli* and *Novomessor albisetosus*. *Insectes*

1145   *Sociaux*, **27**, 148–156.

1146 Wiens J.J. (2007) Global patterns of diversification and species richness in

1147   amphibians. *The American Naturalist*, **170**, S86–106.

1148 Wiens J.J. & Donoghue M.J. (2004) Historical biogeography, ecology and species

1149   richness. *Trends in Ecology and Evolution*, **19**, 639–644.

1150 Wiens J.J. & Graham C.H. (2005) Niche conservatism: integrating evolution,

1151   ecology, and conservation biology. *Annual Review of Ecology, Evolution, and*

1152   *Systematics*, **36**, 519–539.

1153 Willig M.R., Kaufman D.M., & Stevens R.D. (2003) Latitudinal gradients of

1154   biodiversity: pattern, process, scale, and synthesis. *Annual Review of Ecology,*

1155   *Evolution, and Systematics*, **34**, 273–309.

1156 Wing S.L. (1987) Eocene and Oligocene floras and vegetation of the rocky

1157   mountains. *Annals of the Missouri Botanical Garden*, **74**, 748–784.

1158 Wolfe J.A. (1975) Some aspects of plant geography of the northern hemisphere

1159   during the Late Cretaceous and Tertiary. *Annals of the Missouri Botanical*

1160   *Gardens*, **62**, 264–279.

1161   Yoder A.D. & Nowak M.D. (2006) Has vicariance or dispersal been the predominant

1162   biogeographic force in Madagascar? Only time will tell. *Annual Review of*

1163   *Ecology, Evolution, and Systematics*, **37**, 405–431.

1164   Yu Y., Harris A.J., Blair C., & He X. (2015) RASP (Reconstruct Ancestral State in

1165   Phylogenies): a tool for historical biogeography. *Molecular Phylogenetics and*

1166   *Evolution*, **87**, 46–49.

1167   Zachos J., Pagani M., Sloan L., Thomas E., & Billups K. (2001) Trends, rhythms, and

1168   aberrations in global climate 65 Ma to present. *Science*, **292**, 686–693.

1169

Supporting Information

1171   Additional Supporting Information may be found in the online version of this article:

1172

1173   Appendix S1. List of valid Stenammini species and their latitudinal midpoints.

1174   Appendix S2. Voucher information for all specimens used in the phylogeny.

1175   Appendix S3. Sequencing and assembly statistics.

1176   Appendix S4. Results from matrix-filtering experiments.

1177   Appendix S5. Additional trees from RAxML, ExaBayes, and ASTRAL analyses.

1178   Appendix S6. Complete results for divergence dating, biogeography and habitat

1179   reconstruction.

1180   Appendix S7. Additional diversification rate results.

1181

DATA ACCESSIBILITY

1183   All raw sequence data are available from the NCBI Sequence Read Archive (upon

1184   acceptance). The concatenated Filter90 alignment and corresponding ML tree are

1185   available at TreeBASE (upon acceptance).

1186

1187 **BIOSKETCH**

1188

1189 **Michael Branstetter** was recently a postdoctoral scholar at the Smithsonian

1190 Institution (NMNH) and is now a postdoc at the University of Utah. He is broadly

1191 interested in the evolution of ants and other social Hymenoptera, with an emphasis on

1192 the Neotropical region. His research combines phylogenetic systematics,

1193 biogeography, and macroevolution to better understand the origin and maintenance of

1194 biodiversity.

1195

1196 Author contributions: All authors helped design the study and revise the manuscript.

1197 M.G.B. performed all lab work and analyses and drafted the manuscript.

1198

1199

1200   **TABLES**

1201   **Table 1.** Results from divergence dating, biogeography, and habitat reconstruction.
1202   Node numbers correspond to the numbers in Fig. 4c. Biogeographic areas: Nearctic
1203   (A), Neotropics (B), Palearctic (C), Afrotropics (D), Indomalaya (E), Australasia (F).
1204   Habitats: temperate wet (A), temperate dry (B), tropical wet (A), tropical dry (B).
1205

Node #	Node Name	Age (Ma)	95% HPD (Ma)	Biogeo	Habitat
1	Stenammini	53	46-60	AC	AB
2	*Stenamma*	41	31-51	AC	A
3	HOC+MAC *Stenamma*	28	21-36	AC	AC
4	HOC *Stenamma*	24	18-32	AC	A
10	MAC *Stenamma*	23	16-30	AB	C
14	*Novomessor+Aphaenogaster*	51	44-58	A	AB
15	"Novomessor" clade	22	16-29	AB	BD
16	*Novomessor*	14	9-19	AB	BD
18	*Veromessor*	11	8-15	A	D
19	"Deromyrma"+*Aphaenogaster*	43	36-51	AC	AB
20	"Deromyrma" clade	41	34-48	AC	AC
21	New World "Deromyrma"	12	7-19	B	C
22	Old World "Deromyrma"	30	22-37	CE	AC
28	*Goniomma+Aphaenogaster*	38	30-45	C	AB
29	"Goniomma" clade	15	11-20	C	B
30	"Aphaenogaster" clade	17	13-22	C	AB

1223

1224   **Table 2.** Average speciation and extinction rates estimated in BAMM for key groups
1225   of taxa. Node numbers correspond to the numbers in Fig. 4c. Note that rates are
1226   similar except for taxon groups that include the "Aphaenogaster" clade, which has a
1227   significantly increased rate. HOC: Holarctic Clade. MAC: Middle American Clade.
1228

Node #	Lineage	λ Mean	μ Mean
1	all Stenammini	0.1744	0.0430
1	no "Aphaenogaster" clade	0.1226	0.0219
30	"Aphaenogaster" clade	0.3627	0.1199
41	*Stenamma*	0.1241	0.0219
4	HOC *Stenamma*	0.1255	0.0217
10	MAC *Stenamma*	0.1268	0.0217
16	"Novomessor" clade	0.1214	0.0219
20	"Deromyrma" clade	0.1213	0.0219
29	"Goniomma" clade	0.1235	0.0218

1239

1240

1241 **FIGURE LEGENDS**

1242

1243 Figure 1. Midpoint latitude of all extant species of Stenammini binned into 5º

1244 intervals. The plot shows a strong richness peak in the northern temperate zone. (a)

1245 Bars colored by major clade. The "Unknown" category corresponds to the enigmatic

1246 species *Aphaenogaster relicta*. (b) Bars colored by biogeography.

1247

1248 Figure 2. Best maximum likelihood tree depicting relationships among species of

1249 Stenammini. Red dots indicate nodes that received less than 100% bootstrap support

1250 (RAxML) or posterior probability (ExaBayes). All other nodes received maximum

1251 support. Major lineages are highlighted and named as follows: *Stenamma*,

1252 "Novomessor" clade, "Deromyrma" clade, "Goniomma" clade, and "Aphaenogaster"

1253 clade. Ant images from www.antweb.org.

1254

1255 Figure 3. Distribution maps for major lineages of Stenammini. Maps are Mollweide

1256 equal-area projections.

1257

1258 Figure 4. Results from divergence dating, ancestral area inference, habitat

1259 reconstruction, and diversification rate tests. (a) Lineage-through-time plot, with

1260 TreePar tree-wide rate shifts marked by arrows and the Eocene Climatic Optimum

1261 (ECO) and Mid-Miocene Climatic Optimum (MMCO) marked with grey bars. (b)

1262 BAMM speciation-rate-through-time plot showing the overall rate (red line) and the

1263 rate with the "Aphaenogaster" clade excluded. (c) Maximum clade credibility tree

1264 from divergence-dating analysis with BEAST. The red star and red branches indicate

1265   the rate shift inferred by BAMM. The black arrows along the geological timeline

1266   mark the tree-wide rate shifts inferred by TreePar. Circles and squares on nodes

1267   represent inferred ancestral areas and ancestral habitats, respectively. Only key nodes

1268   are marked.

1269

(a) Number of Species vs Latitude, colored by Clade: *Aphaenogaster*, "Deromyrma", "Goniomma", *Messor*, *Novomessor*, *Stenamma*, Uknown

(b) Number of Species vs Latitude, colored by Biogeography: Afrotropical, Australasian, Indomalayan, Nearctic, Neotropical, Palearctic

Pogonomyrmex_occidentalis_EX377
Manica_invidia_EX546
Myrmica_fracticornis_EX545
Adelomyrmex_tristani_EX548
Solenopsis_geminata_EX547
Lachnomyrmex_scrobiculatus_1501
Atta_texana_1479
Lenomyrmex_foveolatus_1500

STENAMMINI

Stenamma

Stenamma_punctiventre_EX309
Stenamma_striatulum_EX335
Stenamma_californicum_cf_EX9
Stenamma_diecki_cf_EX511
Stenamma_snellingi_EX543
Stenamma_msilanum_cf_EX541
Stenamma_debile_EX336
Stenamma_brevicorne_EX109
Stenamma_californicum_EX512
Stenamma_diecki_EX371
Stenamma_dyscheres_EX510
Stenamma_foveolocephalum_EX544
Stenamma_punctatoventre_EX513
Stenamma_impar_EX372
Stenamma_excisum_EX524
Stenamma_lagunum_EX429
Stenamma_brujita_EX433
Stenamma_huachucanum_EX463
Stenamma_lobinodus_EX430
Stenamma_llama_EX133
Stenamma_diversum_EX432
Stenamma_sandinista_EX527
Stenamma_schmidti_EX532
Stenamma_cusuco_EX537
Stenamma_ochrocnemis_EX350
Stenamma_zelum_EX535
Stenamma_expolitum_EX369
Stenamma_alas_EX536
Stenamma_saenzae_EX460
Stenamma_crypticum_EX348
Stenamma_catracho_EX539
Stenamma_ignotum_EX533
Stenamma_callipygium_EX267
Stenamma_felixi_EX370
Stenamma_muralla_EX373
Stenamma_manni_EX530
Stenamma_megamanni_EX368

Novomessor Clade
(Novomessor + Veromessor)

Novomessor_ensifera_EX411
Novomessor_cockerelli_EX504
Novomessor_albisetosa_EX376
Veromessor_lobognathus_EX390
Veromessor_smithi_EX507
Veromessor_lariversi_EX506
Veromessor_pergandei_EX800
Veromessor_chicoensis_EX421
Veromessor_julianus_EX391
Veromessor_andrei_EX505
Veromessor_chamberlini_EX420

Deromyrma Clade
(Tropical Aphaenogaster)

Aphaenogaster_honduriana_EX388
Aphaenogaster_phalangium_EX409
Aphaenogaster_araneoides_EX387
Aphaenogaster_feae_EX415
Aphaenogaster_longiceps_EX410
Aphaenogaster_loriai_EX416
Aphaenogaster_quadrispina_EX386
Aphaenogaster_swammerdami_EX385
Aphaenogaster_mg05_EX516
Aphaenogaster_gonacantha_EX514
Aphaenogaster_mg04_EX515
Aphaenogaster_mg06_EX425

Goniomma Clade
(Goniomma + Oxyopomyrmex)

Goniomma_collingwoodi_EX380
Goniomma_compressisquama_EX700
Goniomma_hispanicum_EX422
Goniomma_baeticum_EX699
Goniomma_blanci_EX520
Oxyopomyrmex_saulcyi_EX501
Oxyopomyrmex_magnus_cf2_EX521
Oxyopomyrmex_magnus_cf1_EX423

Aphaenogaster Clade
(Aphaenogaster + Messor)

Messor_aciculatus_EX427
Messor_sa02_EX424
Messor_barbarus_EX384
Messor_piceus_EX378
Messor_denticornis_EX519
Messor_capensis_EX428
Aphaenogaster_subterranea_EX418
Aphaenogaster_leveillei_EX523
Aphaenogaster_iberica_EX417
Aphaenogaster_sardoa_EX383
Aphaenogaster_striativentris_EX503
Aphaenogaster_gibbosa_EX502
Aphaenogaster_mauritanica_EX522
Aphaenogaster_japonica_EX517
Aphaenogaster_fulva_hpg14
Aphaenogaster_tennesseensis_EX374
Aphaenogaster_famelica_EX426
Aphaenogaster_occidentalis_EX509
Aphaenogaster_texana_EX375
Aphaenogaster_patruelis_EX542
Aphaenogaster_boulderensis_EX412
Aphaenogaster_uinta_EX413
Aphaenogaster_mutica_EX389
Aphaenogaster_megommata_EX379

● < 100% ML or BI Support

Stenamma

Novomessor

Veromessor

Trop. *Aphaenogaster*

Goniomma

Messor

Aphaenogaster

0.02 Substitutions/Site

Stenamma   *Novomessor*   *Veromessor*

"Deromyrma" Clade   "Goniomma" Clade   *Messor*

Aphaenogaster

(a) ECO MMCO — Log Lineages vs Time (Ma)

(b) Speciation Rate vs Time (Ma)

(c) Phylogenetic tree

Key to Biogeography
- Nearctic
- Neotropics
- Palearctic
- Afrotrpics
- Indomalaya
- Australasia

Key to Habitat
- Temperate Wet
- Temperate Dry
- Tropical Wet
- Tropical Dry

Stenamma_punctiventre_EX309
Stenamma_striatulum_EX335
Stenamma_californicum_cf_EX9
Stenamma_debile_EX336
Stenamma_msilanum_cf_EX541
Stenamma_snellingi_EX543
Stenamma_diecki_cf_EX511
Stenamma_brevicorne_EX109
Stenamma_foveolocephalum_EX544
Stenamma_punctatoventre_EX513
Stenamma_impar_EX372
Stenamma_californicum_EX512
Stenamma_dyscheres_EX510
Stenamma_diecki_EX371
Stenamma_excisum_EX524
Stenamma_lagunum_EX429
Stenamma_brujita_EX433
Stenamma_huachucanum_EX463
Stenamma_llama_EX133
Stenamma_lobinodus_EX430
Stenamma_diversum_EX432
Stenamma_schmidti_EX532
Stenamma_sandinista_EX527
Stenamma_cusuco_EX537
Stenamma_ochrocnemis_EX350
Stenamma_zelum_EX535
Stenamma_expolitum_EX369
Stenamma_alas_EX536
Stenamma_saenzae_EX460
Stenamma_catracho_EX539
Stenamma_crypticum_EX348
Stenamma_ignotum_EX533
Stenamma_callipygium_EX267
Stenamma_felixi_EX370
Stenamma_muralla_EX373
Stenamma_megamanni_EX368
Stenamma_manni_EX530
Novomessor_ensifera_EX411
Novomessor_cockerelli_EX504
Novomessor_albisetosa_EX376
Veromessor_smithi_EX507
Veromessor_lobognathus_EX390
Veromessor_pergandei_EX800
Veromessor_lariversi_EX506
Veromessor_chicoensis_EX421
Veromessor_julianus_EX391
Veromessor_chamberlini_EX420
Veromessor_andrei_EX505
Aphaenogaster_honduriana_EX388
Aphaenogaster_phalangium_EX409
Aphaenogaster_araneoides_EX387
Aphaenogaster_feae_EX415
Aphaenogaster_longiceps_EX410
Aphaenogaster_quadrispina_EX386
Aphaenogaster_swammerdami_EX385
Aphaenogaster_mg05_EX516
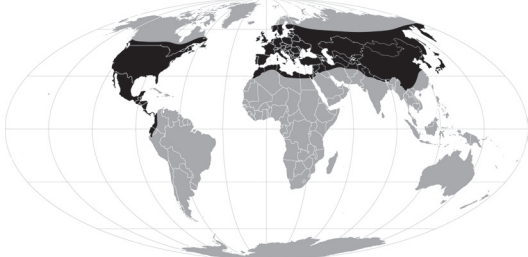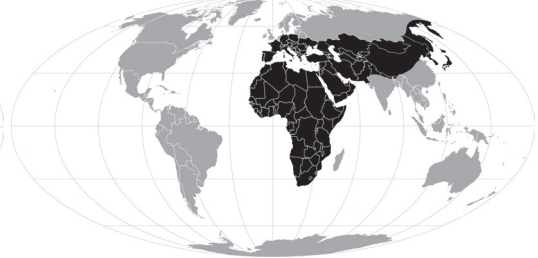Aphaenogaster_gonacantha_EX514
Aphaenogaster_mg06_EX425
Aphaenogaster_mg04_EX515
Goniomma_compressisquama_EX700
Goniomma_collingwoodi_EX380
Goniomma_hispanicum_EX422
Goniomma_baeticum_EX699
Goniomma_blanci_EX520
Oxyopomyrmex_saulcyi_EX501
Oxyopomyrmex_magnus_cf2_EX521
Oxyopomyrmex_magnus_cf1_EX423
Messor_aciculatus_EX427
Messor_sa02_EX424
Messor_barbarus_EX384
Messor_piceus_EX378
Messor_denticornis_EX519
Messor_capensis_EX428
Aphaenogaster_subterranea_EX418
Aphaenogaster_leveillei_EX523
Aphaenogaster_sardoa_EX383
Aphaenogaster_iberica_EX417
Aphaenogaster_striativentris_EX503
Aphaenogaster_mauritanica_EX522
Aphaenogaster_gibbosa_EX502
Aphaenogaster_japonica_EX517
Aphaenogaster_fulva_HPG14
Aphaenogaster_tennesseensis_EX374
Aphaenogaster_famelica_EX426
Aphaenogaster_texana_EX375
Aphaenogaster_occidentalis_EX509
Aphaenogaster_patruelis_EX542
Aphaenogaster_boulderensis_EX412
Aphaenogaster_uinta_EX413
Aphaenogaster_mutica_EX389
Aphaenogaster_megommata_EX379

Eocene | Oligocene | Miocene | Pli | Ple

Millions of Years Ago